

## Supporting Information

### **One-Step Treatment of Phosphite-Laden Wastewater: A Single Electrochemical Reactor Integrating Superoxide Radical-Induced Oxidation and Electrocoagulation**

Sheng Liang, Wenxiao Zheng, Liuyi Zhu, Weijian Duan, Chaohai Wei, and Chunhua Feng<sup>\*,†</sup>

The Key Lab of Pollution Control and Ecosystem Restoration in Industry Clusters, Ministry of Education, School of Environment and Energy, South China University of Technology, Guangzhou 510006, PR China

**Section S1 ~ Section S5**

**Figure 1 ~ Figure 13**

---

Corresponding author.

E-mail address: chfeng@scut.edu.cn

## Section S1

**Proof of EO-induced conversion from phosphite to phosphate.** The rapid formation of Fe-based colloids due to the immediate increase in the solution pH in the integrated EO/EC system tends to entrap P species (particularly phosphate); this makes detection of the phosphate in the solution phase difficult. Attempts were made to monitor the variations in the concentrations of phosphate in the solution and solid phases during the initial period (i.e., 5 min), when smaller amounts of colloids might be produced. As illustrated in [Figure S2](#), a certain amount of phosphate, closely related to the drop in the aqueous concentration of phosphite ([Figure 1](#)), was detected in the solution. This observation indicates that the reactive species originating from the reaction between electrogenerated O<sub>2</sub> and Fe(II) is effective in oxidizing phosphite to phosphate in the solution. The aqueous concentration of phosphate reached a maximum value and then declined due to its adsorption and coprecipitation onto the increasing amount of Fe precipitates as the reaction continued. The concentration of phosphate in the solid increased rapidly with increasing reaction time. The sum of the phosphate concentrations in both phases was close to the decrease in phosphite concentration in the aqueous phase, providing evidence of the EO-induced conversion from phosphite to phosphate.

## Section S2

**Test of the EC effect on the removal of phosphate in comparison to phosphite.** Control tests were conducted to demonstrate that the EC process is capable of removing phosphate from the aqueous phase, but it removes only a small proportion of the phosphite present, as shown in [Figure S3](#). To exclude the influence of EO, the experiments were undertaken in the absence of oxygen and without the MMO anode.

It was found that the EC system substantially decreased the concentration of phosphate, with less than 100  $\mu\text{M}$  remaining after 20 min. In contrast, for the same system, only 9.11% of phosphite disappeared after 60 min.

### Section S3

**Effect of the presence of scavenger on the EC process.** The influence of the presence of scavengers on the EC process was examined. The partitions of Fe(II), Fe(III), P(III), and P(V) in the aqueous and solid phases were obtained in the EO/EC system (MMO anode, 100 mA; Fe anode, 100 mA; reaction time, 60 min) in the absence and presence of scavengers including TBA, EtOH, DMSO, and TEMPOL. As shown in [Figure S13a](#), the partitions of Fe(II) and Fe(III) varied insignificantly for all the treatment and quenching experiments. [Figure S13b](#) shows that the phosphite disappearing from the aqueous phase was primarily transferred to phosphate in the solid phase, and negligible aqueous phosphate was detected in all the tested scenarios. These results suggest that the presence of a scavenger primarily affects the EO process rather than the EC process; otherwise, more phosphate would have been available in the solution.

### Section S4

**Experiments demonstrating phosphite oxidation by  $\bullet\text{O}_2^-$  using an established superoxide-generating process.** A control experiment was performed to verify phosphite oxidation by  $\bullet\text{O}_2^-$  using an established superoxide-generating system. The  $\bullet\text{O}_2^-$  was attained via photolysis (irradiation time of 1 min, wavelength of 254 nm) of an oxygen-saturated solution (200 mL) containing 41.0 mM acetone, 12.0 M ethanol, 15.0  $\mu\text{M}$  diethylenetriaminepentaacetic acid (DTPA), and 1.0 mM borate buffer.<sup>1</sup>

Subsequently, 1000  $\mu\text{M}$  phosphite was added to the solution containing  $\bullet\text{O}_2^-$  species (its concentration was about 30~70  $\mu\text{M}$ ),<sup>1</sup> and the pH value was adjusted to 7.0 by 0.1 M NaOH. After 5 min of reaction, the concentration of generated phosphate was measured and found to be  $33.8 \pm 7.5 \mu\text{M}$ . For comparison, the experiment was also undertaken with the same solution but without irradiation. Under this condition, no  $\bullet\text{O}_2^-$  was generated and accordingly no phosphate was formed. These results provide evidence of the capacity of  $\bullet\text{O}_2^-$  to oxidize phosphite to phosphate.

## Section S5

**Determination of zeta potential of Fe precipitates before and after P adsorption.** The zeta potential of Fe precipitates was measured using the Litesizer™ 500 (Anton-Paar Instruments, Austria). Three runs were conducted for each sample and the average value was reported. For the sample collected from the EO/EC system (MMO anode, 100 mA; Fe anode, 100 mA; reaction time, 60 min) in the absence of P, the zeta potential was  $-8.2 \text{ mV}$ ; the negative value is due to the hydroxyl groups on the Fe colloids. This data is in agreement with data recorded for Fe-based minerals at alkali pH.<sup>2</sup> The zeta potential of the sample collected from the same system in the presence of P was  $-25.3 \text{ mV}$ ; this lower value is expected owing to the presence of negatively charged ions (i.e., phosphate). These results indicate that the mechanism governing adsorption of P on the EC-induced Fe precipitates is not completely attributable to electrostatic force; the surface precipitation of P with the Fe(III) hydroxides should also make an important contribution.<sup>2,3</sup>

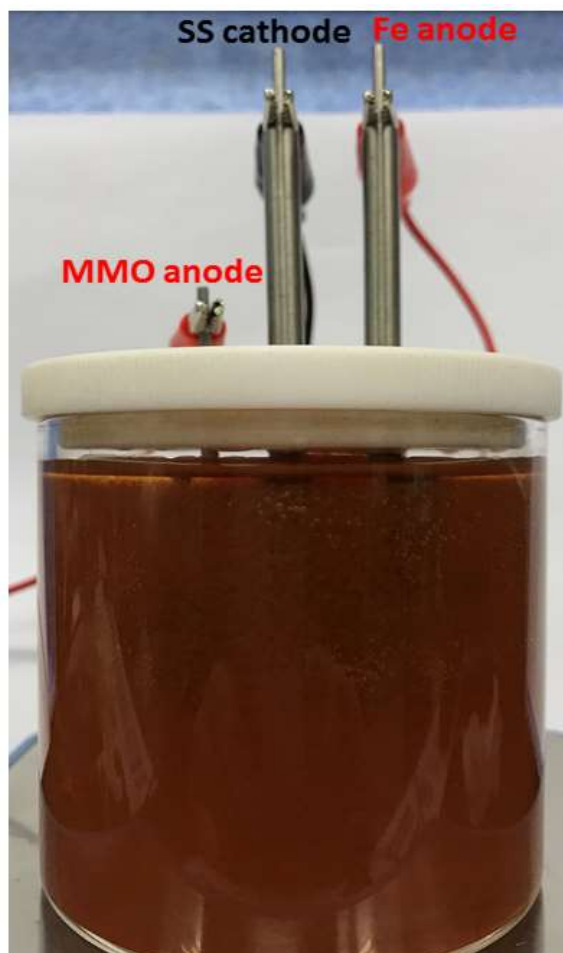


**Figure S1.** Picture of the electrochemical reactor integrating two anodes (a Fe plate and a MMO plate) and a stainless steel (SS) cathode.

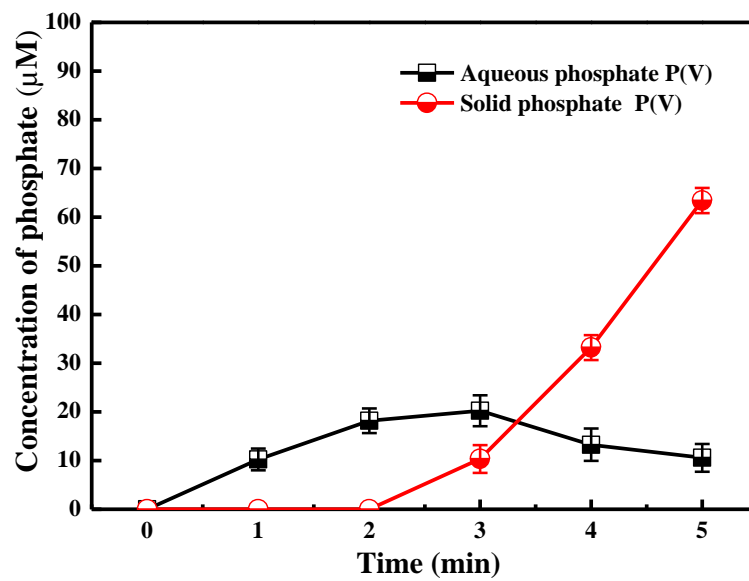


**Figure S2.** Time course of phosphate concentrations in the aqueous and solid phases in the integrated EO/EC systems (MMO anode, 100 mA; Fe anode, 100 mA; reaction time, 5 min).

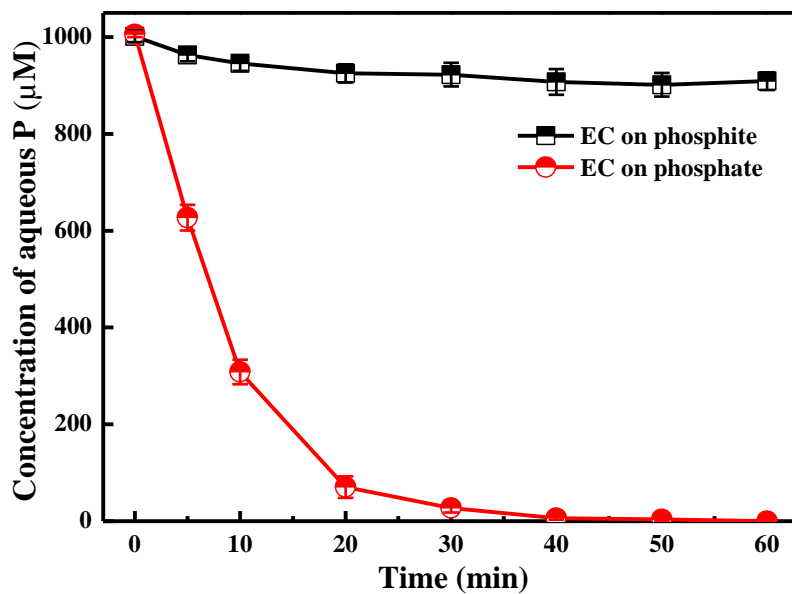


**Figure S3.** Time course of phosphite and phosphate concentrations in the EC systems when the MMO anode was absent and the current applied to the Fe anode was fixed at 100 mA. The initial concentration of phosphite was 1000  $\mu\text{M}$  and initial pH was 4.0. The reaction time was 60 min.

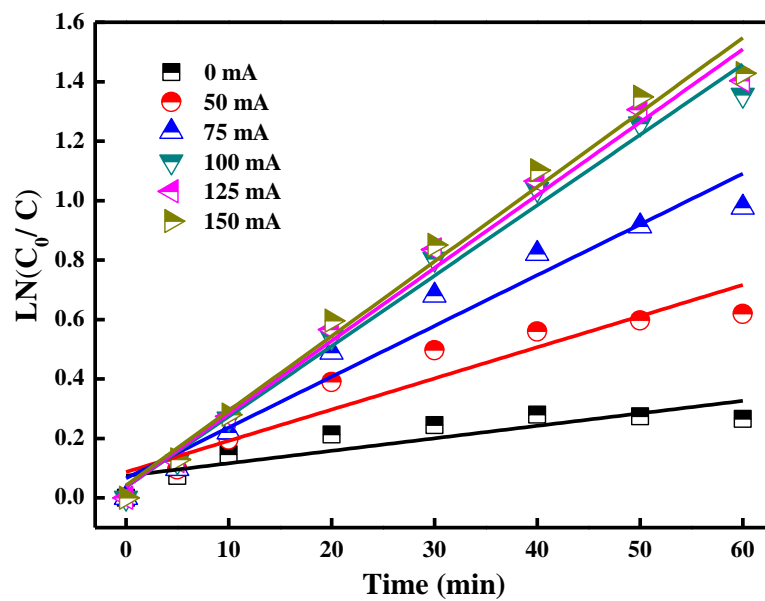


**Figure S4.** First-order kinetic fitting of decay in phosphite concentration by the EO/EC treatments. For these experiments, the current applied to the MMO anode was varied and the current to the Fe anode was fixed at 100 mA.

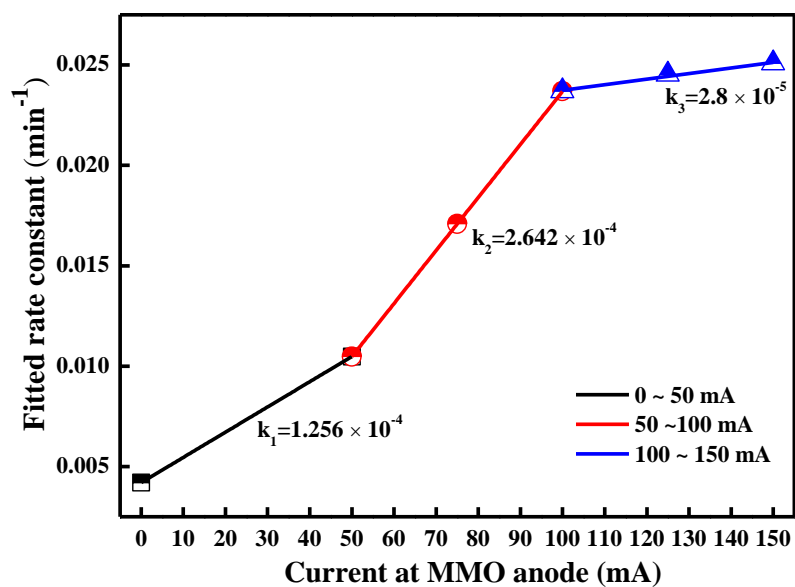


**Figure S5.** Changes in the apparent rate constant as a function of the current at the MMO anode.

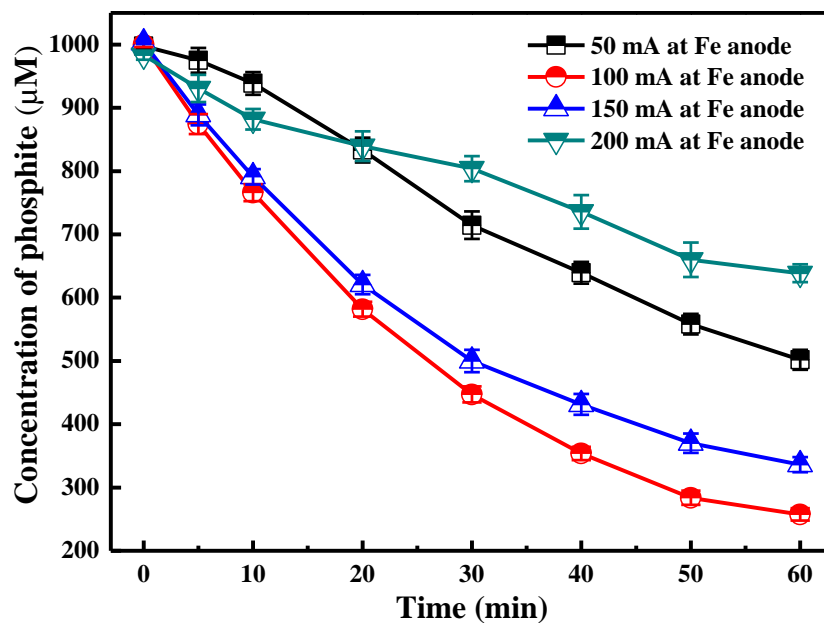


**Figure S6.** Effect of the current (at the Fe anode) on the time course of phosphite concentrations during the EO/EC treatment. The current at the MMO anode was fixed at 100 mA.

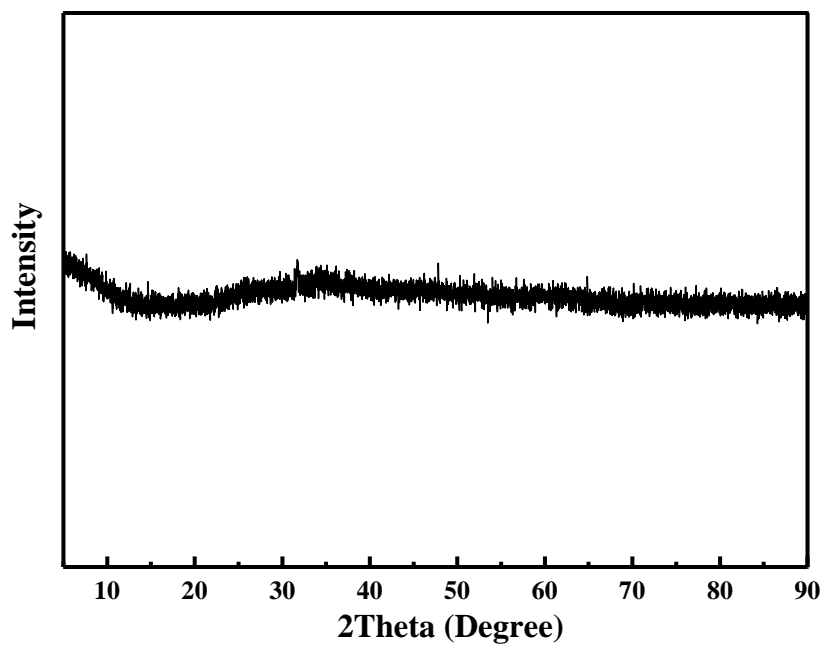


**Figure S7.** XRD pattern of the precipitate generated in the EO/EC system. Experiment conditions: 100 mA at the MMO anode, 100 mA at the Fe anode, initial concentration of 1000  $\mu\text{M}$  phosphite, initial pH of 4.0, and operation time of 60 min.

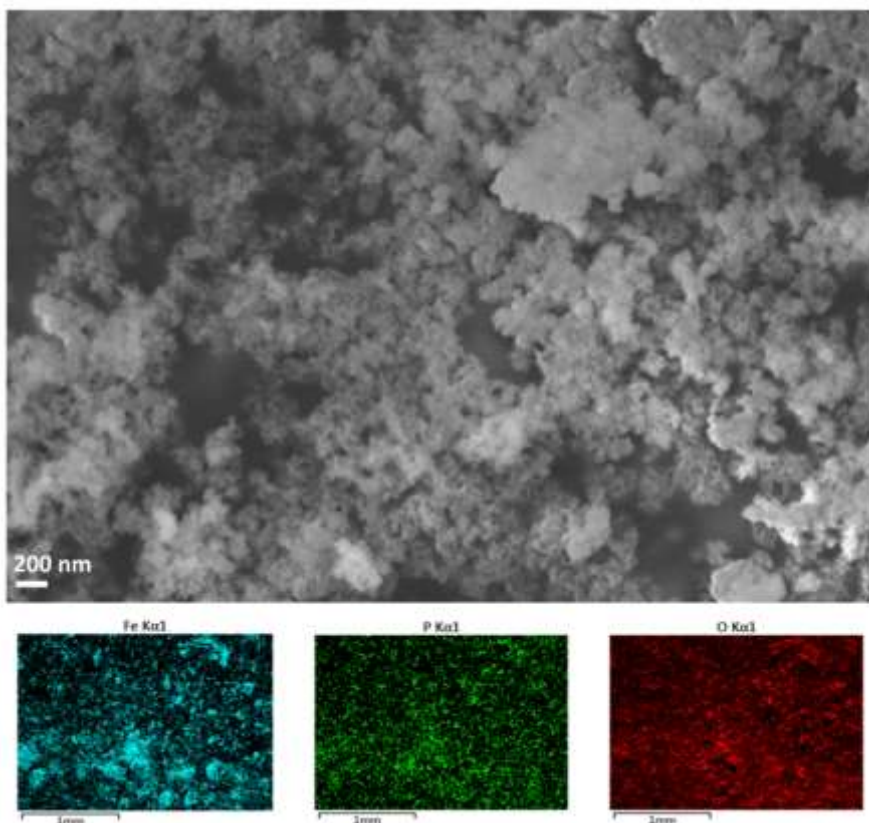


**Figure S8.** SEM image and elemental mappings (Fe, P, O) of the precipitate generated in the EO/EC system. Experiment conditions: 100 mA at the MMO anode, 100 mA at the Fe anode, initial concentration of 1000  $\mu\text{M}$  phosphite, initial pH of 4.0, and operation time of 60 min.

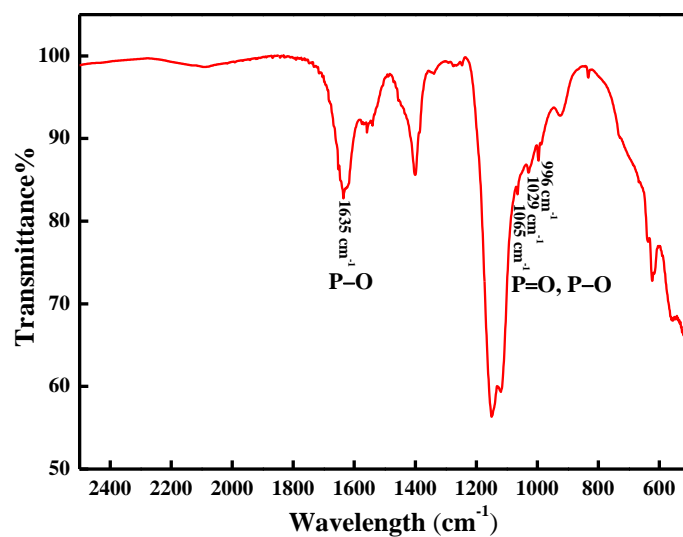


**Figure S9.** FTIR pattern of the precipitate generated in the EO/EC system. Experiment conditions: 100 mA at the MMO anode, 100 mA at the Fe anode, initial concentration of 1000  $\mu\text{M}$  phosphite, initial pH of 4.0, and operation time of 60 min.

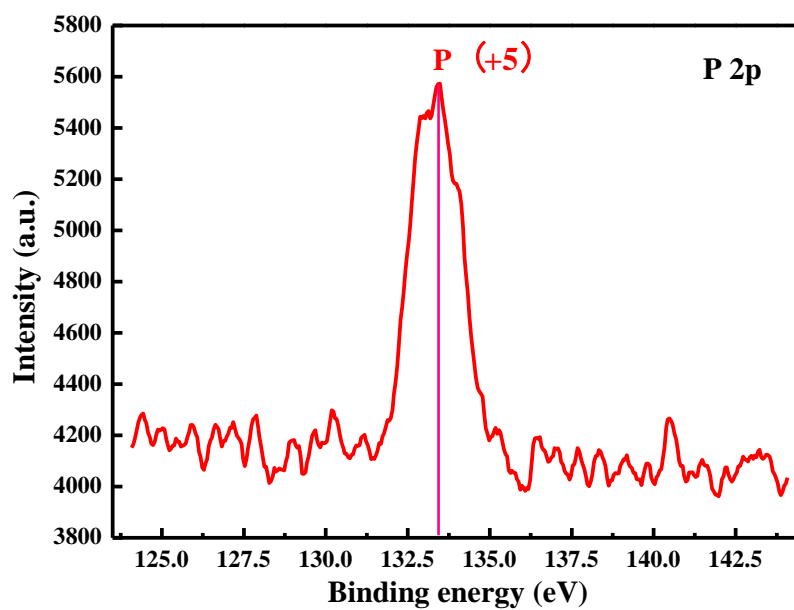


**Figure S10.** P2p XPS of the precipitate generated in the EO/EC system. Experiment conditions: 100 mA at the MMO anode, 100 mA at the Fe anode, initial concentration of 1000  $\mu\text{M}$  phosphite, initial pH of 4.0, and operation time of 60 min.

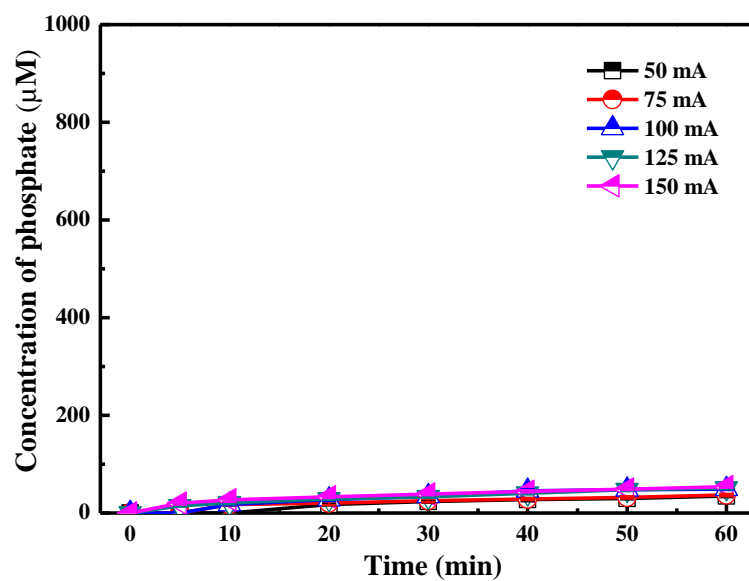


**Figure S11.** Time course of phosphate concentrations in the direct EO systems (the Fe anode is absent) varying in the current (at the MMO anode) from 50 to 150 mA. The initial concentration of phosphite was 1000  $\mu\text{M}$  and initial pH was 4.0.

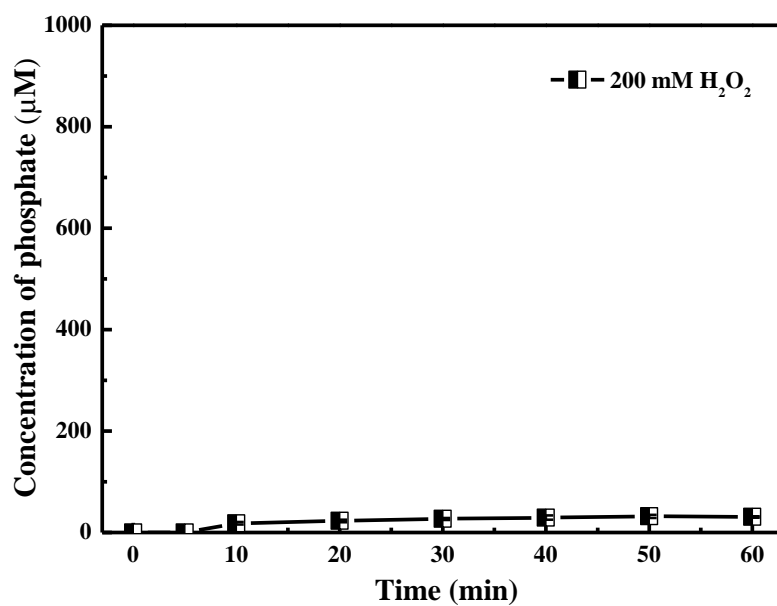


**Figure S12.** Time course of phosphate concentrations for the experiment concerning direct oxidation of phosphite by 200 mM H<sub>2</sub>O<sub>2</sub>. The initial concentration of phosphite was 1000 µM and initial pH was 4.0.

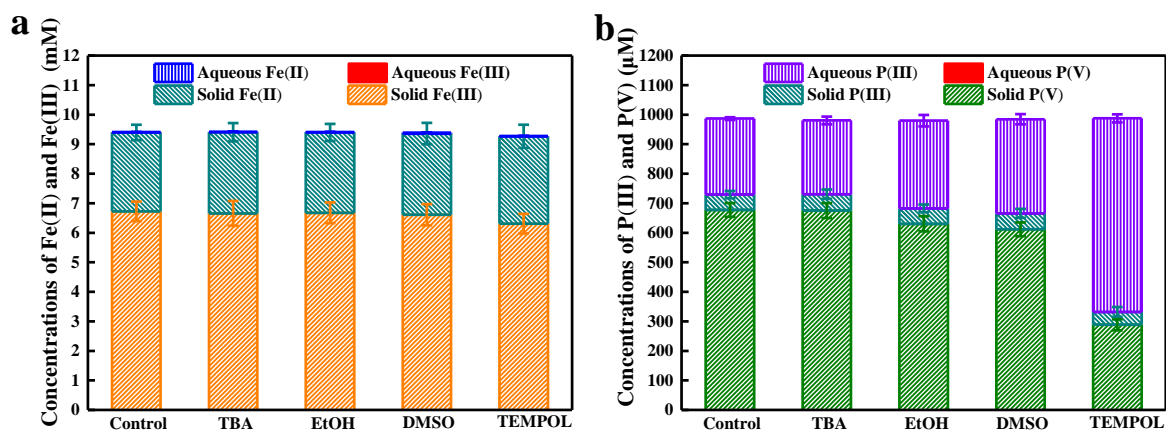


**Figure S13.** Distribution of (a) Fe(II) and Fe(III), and (b) P(III) and P(V) by the end of quenching experiments with scavengers of possible reactive species.

## REFEREMCES

1. Ma, J.; Zhou, H., Yan, S., Song, W., Kinetics studies and mechanistic considerations on the reactions of superoxide radical ions with dissolved organic matter. *Water Res.* **2019**, *149*, 56-64.
2. Li, L.; Stanforth, R., Distinguishing Adsorption and Surface Precipitation of Phosphate on Goethite ( $\alpha$ -FeOOH). *J. Colloid Interface Sci.* **2000**, *230* (1), 12-21.
3. Zhang, J.; Bligh, M. W.; Liang, P.; Waite, T. D.; Huang, X., Phosphorus removal by in situ generated Fe(II): Efficacy, kinetics and mechanism. *Water Res.* **2018**, *136*, 120-130.